

Generic Contrast Agents

Our portfolio is growing to serve you better. Now you have a *choice*.



[VIEW CATALOG](#)

AJNR

This information is current as of May 8, 2025.

Early Detection of Underlying Cavernomas in Patients with Spontaneous Acute Intracerebral Hematomas











A. Bani-Sadr, O.F. Eker, T.-H. Cho, R. Ameli, M. Berhouma, M. Cappucci, L. Derex, L. Mechtouff, D. Meyronet, N. Nighoghossian, Y. Berthezène and M. Hermier

AJNR Am J Neuroradiol 2023, 44 (7) 807-813

doi: <https://doi.org/10.3174/ajnr.A7914>

<http://www.ajnr.org/content/44/7/807>

Early Detection of Underlying Cavernomas in Patients with Spontaneous Acute Intracerebral Hematomas

 A. Bani-Sadr,  O.F. Eker,  T.-H. Cho,  R. Ameli,  M. Berhouma,  M. Cappucci,  L. Derex,  L. Mechtouff, D. Meyronet,  N. Nighoghossian,  Y. Berthezène, and  M. Hermier



ABSTRACT

BACKGROUND AND PURPOSE: Early identification of the etiology of spontaneous acute intracerebral hemorrhage is essential for appropriate management. This study aimed to develop an imaging model to identify cavernoma-related hematomas.

MATERIALS AND METHODS: Patients 1–55 years of age with acute (≤ 7 days) spontaneous intracerebral hemorrhage were included. Two neuroradiologists reviewed CT and MR imaging data and assessed the characteristics of hematomas, including their shape (spherical/ovoid or not), their regular or irregular margins, and associated abnormalities including extralesional hemorrhage and peripheral rim enhancement. Imaging findings were correlated with etiology. The study population was randomly split to provide a training sample (50%) and a validation sample (50%). From the training sample, univariate and multivariate logistic regression was performed to identify factors predictive of cavernomas, and a decision tree was built. Its performance was assessed using the validation sample.

RESULTS: Four hundred seventy-eight patients were included, of whom 85 had hemorrhagic cavernomas. In multivariate analysis, cavernoma-related hematomas were associated with spherical/ovoid shape ($P < .001$), regular margins ($P = .009$), absence of extralesional hemorrhage ($P = .01$), and absence of peripheral rim enhancement ($P = .002$). These criteria were included in the decision tree model. The validation sample ($n = 239$) had the following performance: diagnostic accuracy of 96.1% (95% CI, 92.2%–98.4%), sensitivity of 97.95% (95% CI, 95.8%–98.9%), specificity of 89.5% (95% CI, 75.2%–97.0%), positive predictive value of 97.7% (95% CI, 94.3%–99.1%), and negative predictive value of 94.4% (95% CI, 81.0%–98.5%).

CONCLUSIONS: An imaging model including ovoid/spherical shape, regular margins, absence of extralesional hemorrhage, and absence of peripheral rim enhancement accurately identifies cavernoma-related acute spontaneous cerebral hematomas in young patients.

ABBREVIATION: DVA = developmental venous anomaly

Acute spontaneous intracerebral hematomas are frequent and remain a major cause of morbidity and mortality.¹ The

prognosis and treatment depend on the underlying cause of bleeding. In older patients, primary hemorrhages, due to hypertension or amyloid angiopathy, are the most frequent. The probability of finding a secondary cause, such as vascular malformations, is increased in younger patients.

An etiologic work-up based on imaging is advocated in all patients younger than 55 years of age.^{2,3} In patients presenting with acute spontaneous intracerebral hemorrhage, the shape of the hematoma on imaging performed in the acute phase is correlated with prognosis: Irregular margins may predict hematoma expansion⁴ and have been associated with death and major disability.⁵ In some instances, the shape of the hematoma may also suggest the underlying pathology. Lobar intracerebral hemorrhage with finger-like projections is suggestive of amyloid angiopathy.⁶ Some imaging features, including mixed-aged blood, mulberry-like clusters, and a developmental venous anomaly (DVA) in the vicinity of the hematoma, may suggest an underlying cavernoma. A spherical or ovoid hematoma has sometimes been reported in hemorrhagic

Received January 24, 2023; accepted after revision May 29.

From the Department of Neuroradiology (A.B.-S., O.F.E., R.A., M.C., Y.B., M.H.), Stroke Department (T.-H.C., L.D., L.M., N.N.), Skull Base Surgery Unit (M.B.), Department of Neurosurgery B, and Institute of Pathology East, Neuropathology (D.M.), East Group Hospital, Hospices Civils de Lyon, Bron, France; Creatis Laboratory (A.B.-S., O.F.E., Y.B.), National Center for Scientific Research Unit Mixte de Recherche 5220, Institut National de la Santé et de la Recherche Médicale U 5220, Claude Bernard Lyon I University, Villeurbanne, France; CarMeN Laboratory (T.-H.C., L.M., N.N.), Institut National de la Santé et de la Recherche Médicale U1060, Claude Bernard Lyon I University, Bron, France; Research on Healthcare Performance (L.D.), Institut National de la Santé et de la Recherche Médicale U 1290, Claude Bernard Lyon I University, Domaine Rockefeller, Lyon, France.

A. Bani-Sadr and O.F. Eker contributed equally and are co-first authors.

Please address correspondence to Alexandre Bani-Sadr, MD, Department of Neuroradiology, East Group Hospital, Hospices Civils de Lyon, 59 Boulevard Pinel, 69500 Bron, France; e-mail: apbanisadr@gmail.com



Indicates article with online supplemental data.

<http://dx.doi.org/10.3174/ajnr.A7914>

cerebral cavernomas.^{7,8} However, this characteristic is not mentioned in the widely used MR imaging classification of cavernomas described by Zabramski et al,⁹ and recent reviews on the imaging of acute spontaneous cerebral hemorrhages did not report it as a critical finding.^{10,11} Consequently, the predictive value of a spherical or ovoid hematoma in diagnosing underlying cerebral cavernoma is as yet unknown.

We aimed to assess the radiologic characteristics of hemorrhagic cerebral cavernomas compared with other etiologies in a large series of patients 55 years of age or younger presenting with acute spontaneous intracerebral hematomas. We built and evaluated a radiologic model to predict an underlying cavernoma in case of acute spontaneous intracerebral hematoma.

MATERIALS AND METHODS

We performed a retrospective study in a tertiary hospital (Pierre Wertheimer Hospital, Hospices de Lyon).

Data Availability Statement

Further anonymized data can be provided to qualified investigators on request to the corresponding author.

Ethics Statement

The local ethics committee approved the study and waived the need for informed consent.

Inclusion Criteria

On the basis of our radiology database, we retrieved patients with a diagnosis of symptomatic spontaneous acute cerebral hemorrhage during a 12-year period (January 2010 to December 2021). We included patients 1 year of age and older and 55 years and younger presenting with a first episode of acute-to-early subacute (≤ 7 days) intracerebral hematoma either on CT or MR imaging. Admission imaging had to be available on the PACS to allow multiplanar assessment.

Exclusion Criteria

Patients presenting with intracerebral hematomas lacking imaging data or having poor image quality and no definite or probable etiology after work-up or with traumatic lesions, known brain tumors, hematomas following either IV thrombolytic therapy, interventional neuroradiology, or neurosurgery were excluded. Patients with hematomas of >7 days and intracerebral hematomas with a largest diameter of <10 mm were also excluded.

Etiologies of the Hematoma

The final etiologic diagnosis was determined by consensus between stroke neurologists and neuroradiologists after reviewing all available etiologic work-ups. Etiologic diagnoses were classified as follows: cerebral aneurysm, arteriovenous shunt (ie, AVM, AVF, AVM draining into a DVA), cerebral cavernoma, cerebral vein thrombosis (ie, direct visualization of thrombi in the cerebral venous system on either contrast-enhanced CT or MR imaging or cerebral angiography), hypertension, probable amyloid angiopathy, spontaneous hemorrhagic transformation of ischemic stroke, reversible vasoconstriction syndrome, posterior reversible encephalopathy syndrome, pseudoaneurysm in the setting of infective endocarditis, other vasculopathies (ie, Moyamoya,

vasculitis), neoplasms with acute hemorrhagic presentation, and toxic or coagulation disorders.

For cavernomas, diagnosis was made on the basis of either histopathology^{12,13} or follow-up.¹⁴ Mixed vascular lesions with both cavernous components and capillary telangiectasia at histopathology were classified as cavernomas. Follow-up-based diagnoses were established by consensus after review of the medical files and required a cerebral angiography with negative findings and at least 12 months of follow-up with a favorable clinical course and a typical imaging course of cavernoma as previously described.^{9,14}

Data Collection

Two senior neuroradiologists (A.B.-S., M.H.) reviewed neuroimaging examinations (CT scanner, 1.5T or 3T MR imaging scanners) at the acute (ie, ≤ 7 days) phase. After undergoing a training period of 100 cases, blinded to clinical data and final diagnosis, they reviewed, independently, imaging data of all patients, and discrepancies were settled by consensus.

They classified hematoma shape as being “spherical/ovoid” or not (Fig 1) and as having regular or irregular margins according to the following definition: regular, no angular aspect at any part of the hematoma border; irregular, ≥ 1 angular aspect protruding from any part of the hematoma (Fig 2). Hematomas with lobulated margins without any angular aspect were considered regular (Fig 2). Hematoma location was classified as supratentorial lobar, supratentorial deep, brainstem, cerebellar, or multifocal.

Associated anomalies, including extralesional hemorrhage (ie, intraventricular, subarachnoid, subdural), peripheral rim enhancement, evidence of blood-breakdown products of varying stages, DVA, arteriovenous shunt, and aneurysm, were assessed after analysis of all available imaging data. Radiologic signs of small-vessel disease were also evaluated (microbleeds on T2* and white matter disease with a total Fazekas score of ≥ 2 using FLAIR or CT when MR imaging was not available¹⁵).

Whenever possible, hematoma shape and margins were evaluated on T2*-weighted MR imaging performed in the acute phase, and on T1 and T2 FLAIR sequences when susceptibility artifacts obscured the margins. Plain CT was used when MR imaging data were not available. Volumes were obtained by measuring hematoma diameters and calculated using the ABC/2 score.¹⁶

In case of multiple acute hematomas, the analysis focused on the largest one.

Baseline demographic and clinical characteristics, including medications, patient history, and Glasgow Coma Scale score were collected from the medical records, blinded to imaging data.

Statistical Analysis

Data are presented as counts (percentages) for binary variables and medians (interquartile range) for continuous variables because none were assumed to have normal distributions. Interrater agreement for radiologic characteristics was assessed using the Cohen κ coefficient. Descriptive statistics were performed using parametric or nonparametric tests as appropriate. The study population was randomly split into 2 parts to provide a training sample (50%) and a validation sample (50%). Using the training sample, we performed univariate logistic regression to evaluate putative predictive

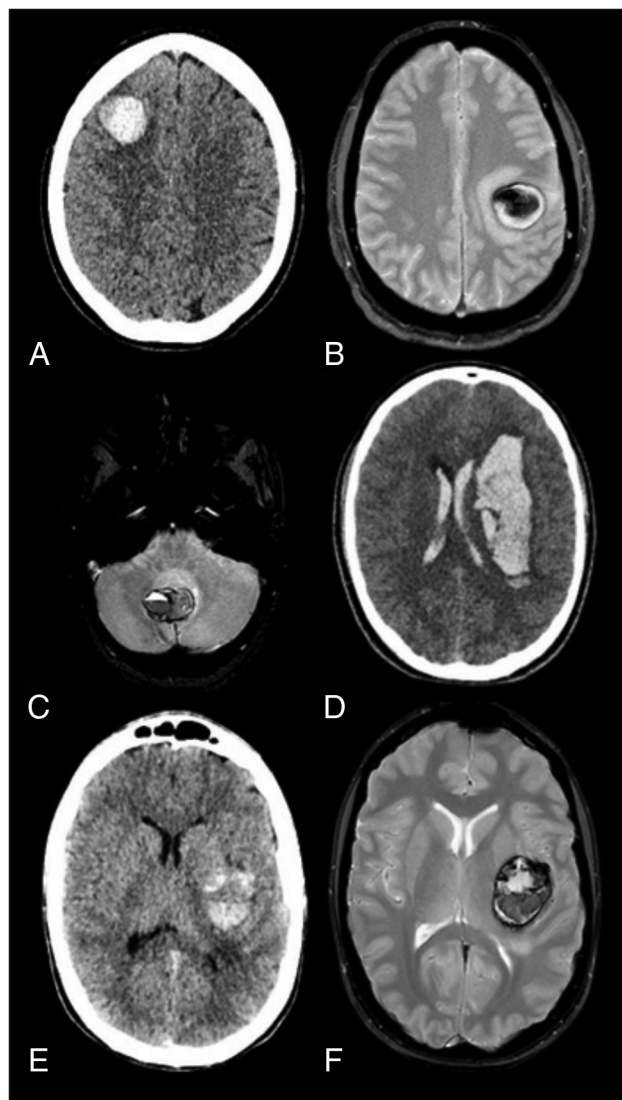


FIG 1. Assessment of hematoma shape. A, Spherical, acute lobar hematoma on plain CT of a patient with a pathologically proved hemorrhagic cerebral cavernoma. B, Spherical lobar hematoma on T2*-weighted imaging in a patient with pathologically proved hemorrhagic cerebral cavernoma. C, Ovoid cerebellar hematoma on T2*-weighted imaging of a patient with pathologically proved hemorrhagic cavernoma. D, Plain CT obtained at admission in a patient with an angiographically proved cerebral AVM. The elongated shape of the hematoma did not fulfill the criteria spherical or ovoid. Its margins were considered irregular because angular aspects were present. It was associated with intraventricular hemorrhage. E and F, Hemorrhagic cerebral cavernoma. Both plain CT (D) and T2* MR images (E) were available to assess the hematoma shape. The hematoma shape was classified as spherical/ovoid on the basis of MR imaging.

factors of underlying cavernomas. A multivariable model was subsequently built using a forward selection with a *P* value threshold of .05. A decision tree including these variables was constructed using a recursive partitioning method (package *rpart*; ¹⁷ <https://www.rdocumentation.org/packages/rpart/versions/4.1.19>). Briefly, this method recursively assesses all possible splits to provide the optimal combination to distinguish hemorrhagic cavernomas from other causes of hematoma. In addition, it is not affected by

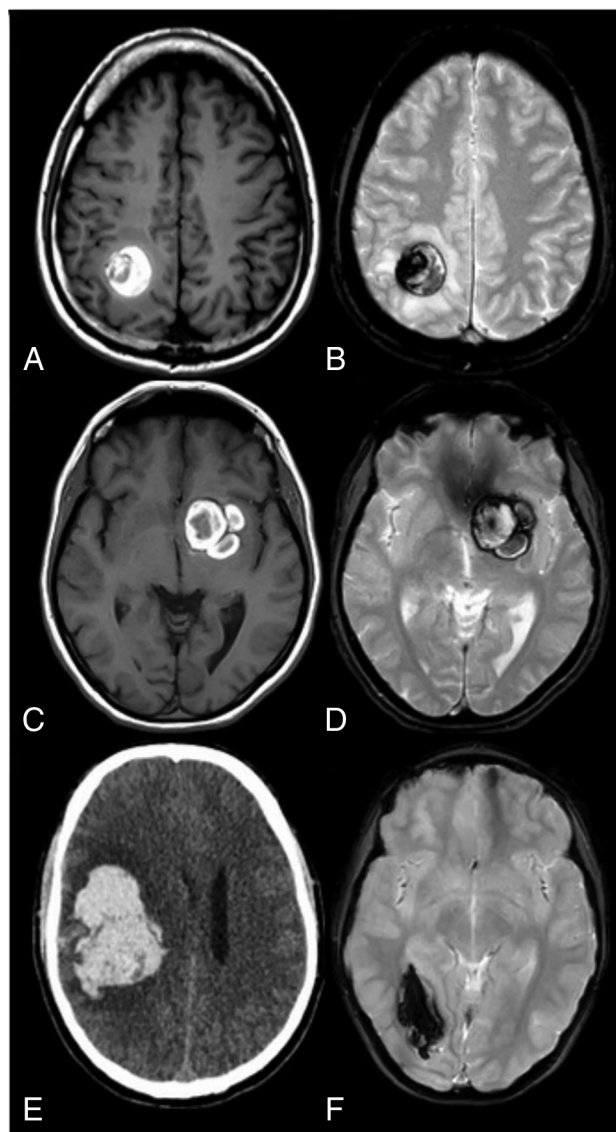


FIG 2. Assessment of hematoma margins. A and B, T1- and T2*-weighted MR imaging shows a hematoma with regular margins in a patient with pathologically proved hemorrhagic cavernoma in the setting of familial cavernomatosis. C and D, T1 and T2*-weighted MR imaging shows a hematoma in a patient with a pathologically proved cerebral cavernoma. The lesion was multiloculated with bumpy borders. The margins were classified as regular because no angular aspect was present in any part of the lesion. Hematoma with irregular margins presenting with angular aspects on plain CT (E) and T2*-weighted MR imaging (F) in 2 patients with arteriovenous shunts proved by cerebral angiography.

multicollinearity effects and correlation among variables. Using the validation sample, we assessed the performance (accuracy, sensitivity, specificity, negative and positive predictive values) of this decision tree by means of a 10-fold cross-validation. The performance of the model was assessed in the whole validation population and among the validation population in patients 18 years of age or younger.

A 2-sided *P* value < .05 was considered statistically significant. All statistical analyses were performed with the R statistical and computing software, Version 3.2.1 (<http://www.r-project.org/>).

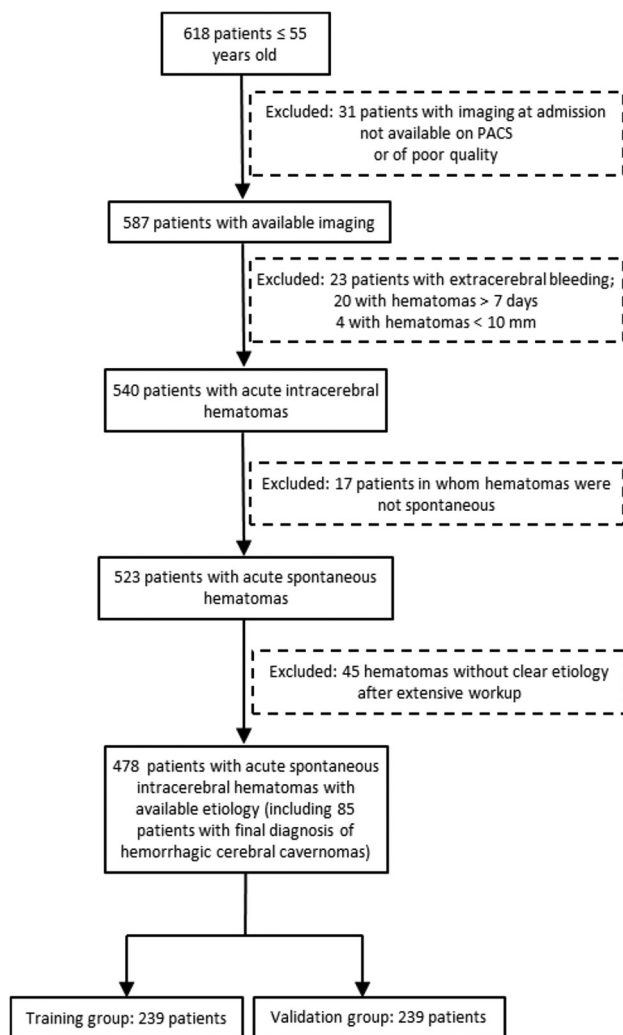


FIG 3. Flowchart of study population.

RESULTS

Descriptive Analysis of the Population

During the study period, we identified 618 patients with a suggestion of acute spontaneous intracerebral hematoma based on imaging reports. One hundred forty subjects were excluded from the study: Thirty-one had unavailable or poor-quality imaging, 23 had purely extracerebral hemorrhages, 20 had hematomas of >7 days, 4 had infracentrimetric hematomas, 45 had no definite etiology at work-up, and in 17, the hematoma was not spontaneous (trauma, surgery, IV thrombolysis). Finally, 478 patients met the inclusion and exclusion criteria. The patient flowchart is shown in Fig 3.

The median age of the study population was 41 years (interquartile range, 26.0–49.0 years), and 259 (54.2%) were men. The Online Supplemental Data detail the number of subjects included for each hematoma etiology and the imaging modalities available for each.

Among them, 85 patients (17.8%) had hemorrhagic cavernomas. The diagnosis of cavernoma was histologically proved in 55 patients, and the remaining 30 patients had at least 12 months of clinical and MR imaging follow-up. Among patients with cavernomas, 27 (31.8%) underwent DSA in the acute phase despite negative findings on noninvasive angiography.

Interrater agreement was good for all radiologic characteristics with a κ coefficient ranging from 0.77 to 0.96. Descriptive clinical and radiologic characteristics of the study population are presented in the Online Supplemental Data. The following characteristics of intracerebral hematomas were associated with cavernomas: spherical or ovoid shape, regular margins, evidence of blood products of varying ages within the lesion, absence of extralesional hemorrhage, absence of peripheral rim enhancement, presence of a DVA near the hematoma, smaller hematoma volume, and no evidence of microbleed or white matter disease. Spherical or ovoid hematomas were significantly smaller (median volume, 6.6 mL; interquartile range, 2.3–12.3 mL, versus 21.6 mL; interquartile range, 9.0–43.1 mL; $P < .001$). Among patients with familial multiple cavernous malformation syndrome ($n = 8$), radiologic characteristics did not significantly differ (all $P \geq .32$) from those of sporadic cavernomas.

Generalized Logistic Regressions

Generalized logistic regressions were performed using the training sample ($n = 239$). At multivariate analysis, the following criteria were significantly associated with cavernomatous etiology: a spherical or ovoid shape, regular margins, absence of extralesional hemorrhage, and absence of peripheral rim enhancement. These parameters were included in the decision tree.

The Table summarizes crude and adjusted ORs of incorporated parameters.

Performance of the Decision Tree Model

When we applied it to the validation sample, the decision tree had the following performance: a diagnostic accuracy of 96.1%, 95% CI, 92.2%–98.4%; a sensitivity of 98.0%, 95% CI, 95.8%–98.9%; a specificity 89.5%, 95% CI, 75.2%–97.0%; a positive predictive value of 97.7%, 95% CI, 94.3%–99.1%; and a negative predictive value of 94.4%, 95% CI, 81.0%–98.5%.

Figure 4 illustrates the decision tree applied to the validation sample.

Among the 71 patients 18 years of age or younger, including 16 with hemorrhagic cavernomas, the decision tree had the following diagnostic performance on the validation sample: a diagnostic accuracy of 96.7% (95% CI, 83.3%–99.9%); a sensitivity of 90.0% (95% CI, 55.5%–99.8%); a specificity 100% (95% CI, 83.9%–100%); a positive predictive value of 100% (95% CI, 66.4%–100%); and a negative predictive value of 95.5% (95% CI, 83.3%–99.9%).

DISCUSSION

Recognizing the underlying etiology of acute spontaneous intracerebral hematomas may be challenging. Cerebral cavernomas are one of the most frequent causes of spontaneous intraparenchymal hematomas in children and young adults.^{18,19} Our study based on a large sample size showed that acute hematomas due to cerebral cavernomas were associated with radiologic characteristics, including a spherical or ovoid shape, regular margins, absence of extralesional hemorrhage, and absence of peripheral rim enhancement. Using these characteristics, we built an accurate radiologic predictive model of hemorrhagic cerebral cavernomas.

Barras et al²⁰ proposed a definition of irregular hematomas, which demonstrated a usefulness in predicting early hematoma

expansion and poor outcome in patients with hemorrhagic stroke.^{4,5,20} The definition we used in the present study differed somewhat from theirs. We assessed hematoma regularity on the whole hematoma (any section, any multiplanar reconstruction plane) rather than specifically on the largest hematoma axial section; and hematomas with any angular aspect arising from their surface were considered here as irregular.

Pathogenetic Hypothesis

We hypothesized that the spherical or ovoid shape and regular margins of hemorrhagic cerebral cavernomas may be due to the presence of a peripheral capsule or pseudocapsule. This capsule, which has often been reported previously,^{21,22} may prevent the extent of bleeding and may contribute to the low incidence of extralesional hemorrhages. According to Abe et al,²² the hematomas arising from cerebral cavernomas often present with a thick capsule, consisting of hyalinized walls and numerous capillaries, and resemble the capsules of chronic subdural hematomas. Although the pathogenesis of the hematoma capsules is not well-understood, it is regarded as the source of intralesional hemorrhage rather than a secondary change after hemorrhage. Most cavernous malformation hemorrhages are not overt and are contained within the margins of the lesion capsule, contrasting with hematomas due to the rupture of other cerebral vascular malformations.^{23,24} However, a peripheral capsule is not always found at the pathologic analysis of hemorrhagic cerebral cavernomas.²⁵ Bleeding within a cavernoma is

believed to occur at low pressure at the capillary level.²⁶ Such low pressure may contribute to explaining why hematomas due to cerebral cavernomas are usually less devastating than those occurring at high pressure, and they typically tend to displace rather than lacerate the surrounding parenchyma.²⁷ In the present study, hematoma volume was lower in patients with cavernomas, and the clinical status assessed by the Glasgow Coma Scale was better than in those with other etiologies of bleeding.

The differential diagnosis of a spherical or ovoid hemorrhagic lesion with regular margins mainly includes hemorrhagic neoplasms. In agreement with previous reports, we found that the absence of peripheral rim enhancement following contrast injection was a useful finding to distinguish cerebral cavernomas from hemorrhagic tumors.^{28,29} Rare cases of “encapsulated intracerebral hematomas” with a spherical shape and regular margins have been reported. Most were chronic, sometimes with peripheral rim enhancement following contrast injection, and were due to cavernomas or following radiosurgery for AVMs or, rarely, aggressive brain tumors.³⁰ In our study, patients with chronic lesions and those with a previous history of cerebral radiation therapy were excluded.

Clinical Implications

Accurate early identification of the etiology of acute spontaneous intracerebral hematomas has several implications. It has a prognostic interest because the morbidity and mortality of cerebral bleeding due to cavernomas are considered lower than in the general setting,³¹ with a 1-month case fatality rate after intracerebral hemorrhage of 2.0%.³² The risk of early hematoma expansion may be lower than in other causes of bleeding. Because cavernomas are angiographically occult malformations, their

Univariate and multivariate logistic regression for the diagnosis of hemorrhagic cavernomas

	Crude OR (95% CI)	P Value	Adjusted OR (95% CI)	P Value
Spherical/ovoid	36.60 (15.89–110.20)	<.001	6.11 (2.64–15.08)	<.001
Regular margins	34.81 (14.99–103.90)	<.001	3.38 (1.44–8.61)	.009
Extralesional hemorrhage	0.06 (0.02–0.15)	<.001	0.39 (0.18–0.76)	.01
Peripheral rim enhancement	0.18 (0.03–0.53)	.009	0.29 (0.13–0.59)	.002

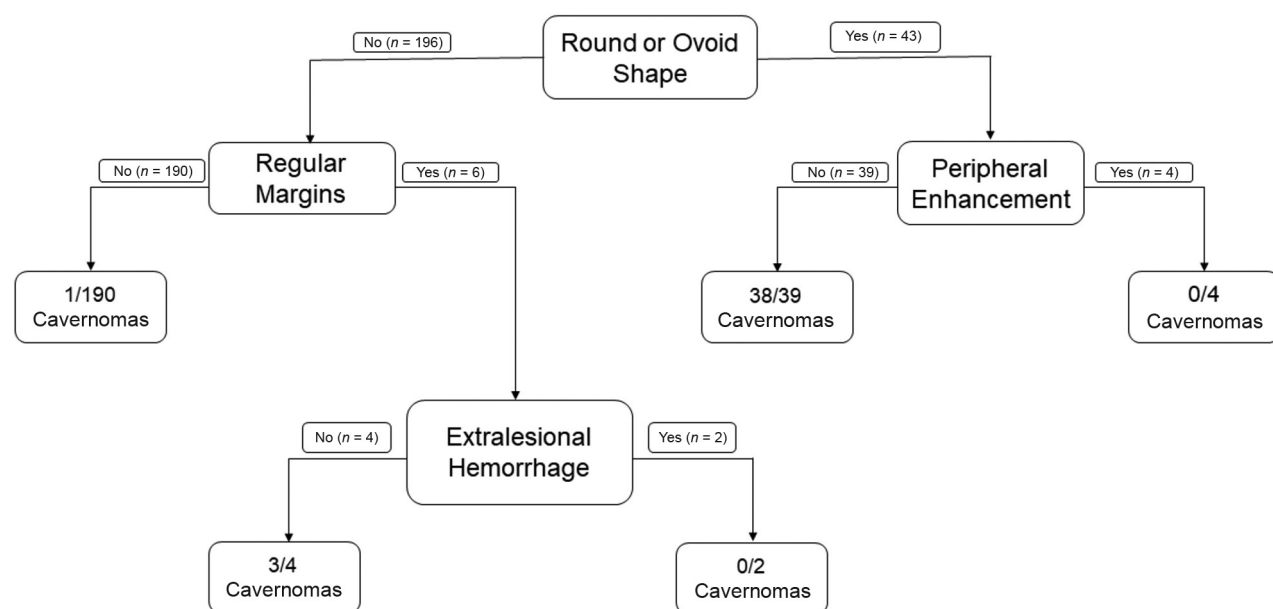


FIG 4. Decision tree model applied to the validation sample.

early recognition may avoid the risks of futile invasive cerebral angiography. Conventional angiography is not recommended in the evaluation of cerebral cavernomas, unless a differential diagnosis of arteriovenous malformation is being considered.³³ Early recognition of symptomatic hemorrhagic cerebral cavernomas may be useful in the accurate enrollment of patients in future trials testing drugs to prevent iterative bleeding.³⁴

Limitations of the Study

This study has limitations. Because our series originates from a third-referral single center with neurosurgical and interventional neuroradiology facilities, our findings may not be representative of the general population. Referral bias could have resulted in a disproportionately high number of patients with vascular malformations. Because we included patients 55 years of age or younger, our model may, therefore, not be appropriate in older patients. The criterion standard for the diagnosis of hemorrhagic cerebral cavernomas remains histopathology, and in our study, the diagnosis was based on such analyses in 55 of 85 patients; in 30 patients, the diagnosis was established by follow-up.

The diagnostic accuracy of our predictive model was not improved when adding other parameters associated with hemorrhagic cavernomas (ie, evidence of blood products of varying ages within the lesion, presence of a DVA close to the hematoma, smaller hematoma volume, and no evidence of microbleeds or white matter disease). However, this issue might be due to the size of our study population. Indeed, the discovery of a DVA next to a hematoma should suggest a cavernoma as the etiology of the hemorrhage, and a DVA may increase the risk of bleeding from cavernomas.³⁵ The presence of acute hemorrhage might have obscured mixed-aged blood and DVAs in some cases. Moreover, we observed that hematomas due to cavernomas were smaller than in other etiologies, but we could not demonstrate a causal relationship between hematoma size and shape. Finally, we performed an internal validation but not an external validation. A large-scale, multicenter, prospective, external validation of our model is necessary.

CONCLUSIONS

Spontaneous acute intracerebral hemorrhage with spherical or ovoid shape, regular margins, absence of extrasional hemorrhage, and absence of peripheral rim enhancement is highly suggestive of an underlying cerebral cavernoma in patients 55 years of age or younger. A decision tree including these parameters seems to have excellent performance and requires further validation because it may have major implications and prognostic interest in clinical practice.

Disclosure forms provided by the authors are available with the full text and PDF of this article at www.ajnr.org.

REFERENCES

- Gross BA, Jankowitz BT, Friedlander RM. **Cerebral intraparenchymal hemorrhage: a review.** *JAMA* 2019;321:1295–303 [CrossRef Medline](#)
- Kamel H, Navi BB, Hemphill JC 3rd. **A rule to identify patients who require magnetic resonance imaging after intracerebral hemorrhage.** *Neurocrit Care* 2013;18:59–63 [CrossRef Medline](#)
- Salmela MB, Mortazavi S, Jagadeesan BD, et al; Expert Panel on Neurologic Imaging. **ACR Appropriateness Criteria Cerebrovascular Disease.** *J Am Coll Radiol* 2017;14:S34–61 [CrossRef Medline](#)
- Morotti A, Boulouis G, Dowlatshahi D, et al; International NCCT ICH Study Group. **Standards for detecting, interpreting, and reporting noncontrast computed tomographic markers of intracerebral hemorrhage expansion.** *Ann Neurol* 2019;86:480–92 [CrossRef Medline](#)
- Delcourt C, Zhang S, Arima H, et al; INTERACT2 Investigators. **Significance of hematoma shape and density in intracerebral hemorrhage: the Intensive Blood Pressure Reduction in Acute Intracerebral Hemorrhage Trial study.** *Stroke* 2016;47:1227–32 [CrossRef Medline](#)
- Rodrigues MA, Samarasekera N, Lerpiniere C, et al. **The Edinburgh CT and genetic diagnostic criteria for lobar intracerebral haemorrhage associated with cerebral amyloid angiopathy: model development and diagnostic test accuracy study.** *Lancet Neurol* 2018;17:232–40 [CrossRef Medline](#)
- Mottolese C, Hermier M, Stan H, et al. **Central nervous system cavernomas in the pediatric age group.** *Neurosurg Rev* 2001;24:55–71; discussion 72–73 [CrossRef Medline](#)
- Kurihara N, Suzuki H, Kato Y, et al. **Hemorrhage owing to cerebral cavernous malformation: imaging, clinical, and histopathological considerations.** *Jpn J Radiol* 2020;38:613–21 [CrossRef Medline](#)
- Zabramski JM, Wascher TM, Spetzler RF, et al. **The natural history of familial cavernous malformations: results of an ongoing study.** *J Neurosurg* 1994;80:422–32 [CrossRef Medline](#)
- Kranz PG, Malinzak MD, Amrhein TJ. **Approach to imaging in patients with spontaneous intracranial hemorrhage.** *Neuroimaging Clin N Am* 2018;28:353–74 [CrossRef Medline](#)
- Rindler RS, Allen JW, Barrow JW, et al. **Neuroimaging of intracerebral hemorrhage.** *Neurosurgery* 2020;86:E414–23 [CrossRef Medline](#)
- Tomlinson FH, Houser OW, Scheithauer BW, et al. **Angiographically occult vascular malformations: a correlative study of features on magnetic resonance imaging and histological examination.** *Neurosurgery* 1994;34:792–99; discussion 799–800 [CrossRef Medline](#)
- Frischer JM, Pipp I, Stavrou I, et al. **Cerebral cavernous malformations: congruency of histopathological features with the current clinical definition.** *J Neurol Neurosurg Psychiatry* 2008;79:783–88 [CrossRef Medline](#)
- Flemming KD, Kumar S, Lanzino G, et al. **Baseline and evolutionary radiologic features in sporadic, hemorrhagic brain cavernous malformations.** *AJNR Am J Neuroradiol* 2019;40:967–72 [CrossRef Medline](#)
- Fazekas F, Barkhof F, Wahlund LO, et al. **CT and MRI rating of white matter lesions.** *Cerebrovasc Dis* 2002;13(Suppl 2):31–36 [CrossRef Medline](#)
- Webb AJ, Ullman NL, Morgan TC, et al; MISTIE and CLEAR Investigators. **Accuracy of the ABC/2 score for intracerebral hemorrhage: systematic review and analysis of MISTIE, CLEAR-IVH, and CLEAR III.** *Stroke* 2015;46:2470–76 [CrossRef Medline](#)
- Breiman L, Friedman JH, Olshen RA, et al. *Classification and Regression Trees.* Routledge; 2017
- Boulouis G, Blauwblomme T, Hak JF, et al. **Nontraumatic pediatric intracerebral hemorrhage.** *Stroke* 2019;50:3654–61 [CrossRef Medline](#)
- Goldstein HE, Solomon RA. **Epidemiology of cavernous malformations.** *Handb Clin Neurol* 2017;143:241–47 [CrossRef Medline](#)
- Barras CD, Tress BM, Christensen S, et al; Recombinant Activated Factor VII Intracerebral Hemorrhage Trial Investigators. **Density and shape as CT predictors of intracerebral hemorrhage growth.** *Stroke* 2009;40:1325–31 [CrossRef Medline](#)
- Zabramski JM, Henn JS, Coons S. **Pathology of cerebral vascular malformations.** *Neurosurg Clin N Am* 1999;10:395–410 [CrossRef Medline](#)
- Abe M, Fukudome K, Sugita Y, et al. **Thrombus and encapsulated hematoma in cerebral cavernous malformations.** *Acta Neuropathol* 2005;109:503–09 [CrossRef Medline](#)
- Cordonnier C, Al-Shahi Salman R, Bhattacharya JJ, et al; SIVMS Collaborators. **Differences between intracranial vascular malformation types in the characteristics of their presenting haemorrhages: prospective, population-based study.** *J Neurol Neurosurg Psychiatry* 2008;79:47–51 [CrossRef Medline](#)

24. Ellis JA, Barrow DL. **Supratentorial cavernous malformations.** *Handb Clin Neurol* 2017;143:283–89 [CrossRef Medline](#)
25. Steiger HJ, Markwalder TM, Reulen HJ. **Clinicopathological relations of cerebral cavernous angiomas: observations in eleven cases.** *Neurosurgery* 1987;21:879–84 [CrossRef Medline](#)
26. Little JR, Awad IA, Jones SC, et al. **Vascular pressures and cortical blood flow in cavernous angioma of the brain.** *J Neurosurg* 1990;73:555–59 [CrossRef Medline](#)
27. Flemming KD, Lanzino G. **Cerebral cavernous malformation: what a practicing clinician should know.** *Mayo Clin Proc* 2020;95:2005–20 [CrossRef Medline](#)
28. Sze G, Krol G, Olsen WL, et al. **Hemorrhagic neoplasms: MR mimics of occult vascular malformations.** *AJR Am J Roentgenol* 1987;149:1223–30 [CrossRef Medline](#)
29. Kumar S, Brinjikji W, Lanzino G, et al. **Distinguishing mimics from true hemorrhagic cavernous malformations.** *J Clin Neurosci* 2020;74:11–17 [CrossRef Medline](#)
30. Nishiyama A, Toi H, Takai H, et al. **Chronic encapsulated intracerebral hematoma: three case reports and a literature review.** *Surg Neurol Int* 2014;5:88 [CrossRef Medline](#)
31. Taslimi S, Modabbernia A, Amin-Hanjani S, et al. **Natural history of cavernous malformation: systematic review and meta-analysis of 25 studies.** *Neurology* 2016;86:1984–91 [CrossRef Medline](#)
32. Horne MA, Flemming KD, Su IC, et al; Cerebral Cavernous Malformations Individual Patient Data Meta-analysis Collaborators. **Clinical course of untreated cerebral cavernous malformations: a meta-analysis of individual patient data.** *Lancet Neurol* 2016;15:166–73 [CrossRef Medline](#)
33. Akers A, Al-Shahi Salman R, Awad AI, et al. **Synopsis of guidelines for the clinical management of cerebral cavernous malformations: consensus recommendations based on systematic literature review by the Angioma Alliance Scientific Advisory Board Clinical Experts Panel.** *Neurosurgery* 2017;80:665–80 [CrossRef Medline](#)
34. Awad IA, Polster SP. **Cavernous angiomas: deconstructing a neurosurgical disease.** *J Neurosurg* 2019;131:1–13 [CrossRef Medline](#)
35. Idiculla PS, Gurala D, Philipose J, et al. **Cerebral cavernous malformations, developmental venous anomaly, and its coexistence: a review.** *Eur Neurol* 2020;83:360–68 [CrossRef Medline](#)